Adjuvanticity of a synthetic cord factor analogue for subunit *Mycobacterium tuberculosis* vaccination requires FcRγ–Syk–Card9–dependent innate immune activation

Kerstin Werninghaus,[1,7] Anna Babiak,[1] Olaf Groß,[2] Christoph Hölscher,[3] Harald Dietrich,[1] Else Marie Agger,[4] Jörg Mages,[1] Attila Mocsai,[5] Hanne Schoenen,[7] Katrin Finger,[2] Falk Nimmerjahn,[6] Gordon D. Brown,[8] Carsten Kirschning,[1] Antje Heit,[1] Peter Andersen,[4] Hermann Wagner,[1] Jürgen Ruland,[2] and Roland Lang[1,7]

[1]Institute of Medical Microbiology, Immunology and Hygiene, Technical University Munich, D-81675 Munich, Germany
[2]Department of Hematology, Technical University Munich, 80333 Munich, Germany
[3]Division of Infection Immunology, Research Center Borstel, D-23845 Borstel, Germany
[4]Adjuvant Research, Department of Infectious Disease Immunology, Statens Serum Institute, 2300 Copenhagen, Denmark
[5]Semmelweis University School of Medicine, Budapest H-1089, Hungary
[6]Molecular Medicine, [7]Institute of Clinical Microbiology, University Hospital Erlangen, 91054 Erlangen, Germany
[8]Division of Immunology, CLS, Institute for Infectious Diseases and Molecular Medicine, University of Cape Town, 7925 Cape Town, South Africa

Novel vaccination strategies against *Mycobacterium tuberculosis* (MTB) are urgently needed. The use of recombinant MTB antigens as subunit vaccines is a promising approach, but requires adjuvants that activate antigen-presenting cells (APCs) for elicitation of protective immunity. The mycobacterial cord factor Trehalose-6,6-dimycolate (TDM) and its synthetic analogue Trehalose-6,6-dibehenate (TDB) are effective adjuvants in combination with MTB subunit vaccine candidates in mice. However, it is unknown which signaling pathways they engage in APCs and how these pathways are coupled to the adaptive immune response. Here, we demonstrate that these glycolipids activate macrophages and dendritic cells (DCs) via Syk–Card9–Bcl10–Malt1 signaling to induce a specific innate activation program distinct from the response to Toll-like receptor (TLR) ligands. APC activation by TDB and TDM was independent of the C-type lectin receptor Dectin-1, but required the immunoreceptor tyrosine-based activation motif–bearing adaptor protein Fc receptor γ chain (FcRγ). In vivo, TDB and TDM adjuvant activity induced robust combined T helper (Th)-1 and Th-17 T cell responses to a MTB subunit vaccine and partial protection against MTB challenge in a Card9-dependent manner. These data provide a molecular basis for the immunostimulatory activity of TDB and TDM and identify the Syk–Card9 pathway as a rational target for vaccine development against tuberculosis.

CORRESPONDENCE
Roland Lang:
Roland.Lang@uk-erlangen.de
OR
Jürgen Ruland:
jruland@lrz.tum.de

Tuberculosis causes 2 million deaths per year and is increasingly difficult to treat because of multiple drug resistance. In addition, the existing live vaccine, *Mycobacterium bovis* BCG, lacks efficacy in most developing countries where the major burden of disease occurs (1). This failure has been attributed to exposure to environmental mycobacteria that induces low-level antimycobacterial immunity and blocks the BCG vaccine "take" (2). The development of recombinant *Mycobacterium tuberculosis* (MTB) antigens as subunit vaccines is an attractive strategy, because they are not affected by prior exposure to mycobacteria and, in contrast to BCG, are safe in immunocompromised persons. However, elicitation of protective immunity to intracellular

K. Werninghaus, A. Babiak, and O. Groß and J. Ruland and R. Lang contributed equally to this paper.

The Rockefeller University Press $30.00
J. Exp. Med. Vol. 206 No. 1 89-97
www.jem.org/cgi/doi/10.1084/jem.20081445

pathogens with recombinant subunit vaccines has not been straightforward.

During infection, or vaccination with BCG, the innate immune system recognizes so-called pathogen-associated molecular patterns (PAMPs), resulting in the activation of APCs. PAMPs derived from different classes of pathogens bind to diverse families of pattern recognition receptors that include Toll-like receptors (TLRs), C-type lectins, or NOD-like receptors. These interactions decode pathogen information by triggering distinct signaling pathways to differentially activate APCs, thereby directing the adaptive effector response in a manner that is specifically tailored to the invading microbe. Ligands for TLRs, such as bacterial CpG DNA or LPS, activate signaling via the adaptor protein Myd88 and induce T helper (Th)-1–directing cytokines like IL-12 (3). In contrast, the binding of the β-glucans Curdlan or Zymosan to the C-type lectin receptor Dectin-1 activates the kinase Syk, initiating signaling via the Card9–Bcl10–Malt1 pathway, and it can direct Th-17 differentiation (4, 5). Other immunoreceptor tyrosine-based activation motif (ITAM)–coupling receptors can trigger Syk–Card9 activation in myeloid cells via the adaptor proteins Dap12 or Fc receptor γ chain (FcRγ) (6), but their effects on adaptive immune responses are not known.

Protection against MTB infection requires antigen-specific $CD4^+$ Th-1 T lymphocytes producing IFN-γ, which enables macrophages to kill intracellular mycobacteria (7). The induction of IL-17–producing Th-17 cells after immunization was recently shown to contribute to protection by rapid recruitment of effector cells, including Th-1 cells, to the site of infection (8).

Because recombinant protein antigens usually do not activate APCs, for successful use as subunit vaccines the addition of adjuvants is necessary. The adjuvant most widely used in humans is aluminum hydroxide, which induces antibody responses but only inefficiently primes T cell responses required for control of intracellular infections. CFA, an emulsion made of killed MTB, efficiently induces Th-1 responses in mice, but is too toxic for use in humans. In the search for adjuvants that are both safe and effective, purified PAMPs and their synthetic analogues have been investigated. The mycobacterial cell wall component Trehalose-6,6-dimycolate (TDM), also known as cord factor, has potent inflammatory activity (9) and is used alone or in combination with a TLR4 ligand as an experimental adjuvant (8, 10). The less toxic, synthetic cord factor analogue Trehalose-6,6-dibehenate (TDB; for structures see Fig. S1, available at http://www.jem.org/cgi/content/full/jem.20081445/DC1) (11) induces robust Th-1 immunity after vaccination with the recombinant MTB antigen H1, conferring protection to infection challenge with a reduction in mycobacterial load comparable to the "gold standard" BCG (12, 13). H1 is a fusion of the MTB proteins Ag85B and ESAT-6 that is currently being tested as a subunit vaccine candidate in humans (1). However, the mechanism(s) by which the glycolipid adjuvants TDB and TDM initiate protective T cell immunity, particularly how they activate APCs, are unknown.

Here, we report that the mycobacteria-derived glycolipid TDM and the synthetic adjuvant analogue TDB selectively activate the FcRγ–Syk–Card9 pathway in APC to induce a unique innate immune activation program that directs protective Th-1 and -17 immunity after subunit MTB vaccination.

RESULTS AND DISCUSSION

Priming of IFN-γ and IL-17 production by the adjuvant TDB

To characterize the adjuvant activity of TDB, we first immunized mice with H1 together with TDB or the TLR9 ligand CpG oligodeoxynucleotide (ODN) 1826, and investigated the priming of Th-1 and -17 T cell responses by restimulating lymph node cells with H1 in vitro. Both TDB and CpG induced a robust Th-1 T cell response characterized by profound antigen-specific IFN-γ production (Fig. 1 A). However, only TDB, and not CpG, also activated a strong H1-specific Th-17 T cell response, indicating that this glycolipid has an adjuvant activity that differs fundamentally from that of a classical TLR agonist (Fig. 1 A). Because the immunostimulatory capacity of TDB presumably depends on direct effects on the innate immune system, we next analyzed the ability of TDB to activate APCs in vitro.

TDB and TDM trigger distinct APC activation programs

As an initial readout for cell activation, we used nitric oxide (NO) production from BM-derived macrophages (BMMs; Fig. 1 B). TDB, as well as the cord factor TDM, induced substantial amounts of NO, especially after priming with IFN-γ (Fig. 1 B). However, compared with CpG, the kinetics of TDB-mediated NO production was delayed (Fig. 1 C). To investigate the differences in the effects of TDB and CpG on myeloid cell activation more generally, we next measured global changes in gene expression over time. As expected, both stimuli induced substantial transcriptional reprogramming, again with an overall slower response to TDB (Fig. 1 D). We also observed qualitative differences in gene expression, as a hierarchical clustering revealed TDB-selective (cluster C) or CpG-selective gene induction (cluster D) in addition to common down- and up-regulated target genes (cluster A, B1) and genes induced early by CpG and later by TDB (cluster B2). Selected examples of TDB-induced genes were confirmed at the protein level, validating the microarray data (Fig. S2, available at http://www.jem.org/cgi/content/full/jem.20081445/DC1). We then focused on differentially expressed cytokines that can direct Th cell differentiation (Fig. 1, E–G). IL-12p40 was strongly induced by CpG but not by TDB (Fig. 1 E), whereas IL-6 and IL-1β were expressed transiently after CpG and delayed after TDB treatment (Fig. 1, F and G). Notably, TDB, but not CpG, triggered a significant release of IL-1β into the culture supernatant (Fig. 1 F). We also analyzed the ability of TDB to activate DCs as the most potent APC. We found that TDB caused up-regulation of MHC-II and of the costimulatory molecules CD40, CD80, and CD86 on the cell surface (Fig. 1 H) and triggered cytokine and NO release in DCs in a manner similar to that in

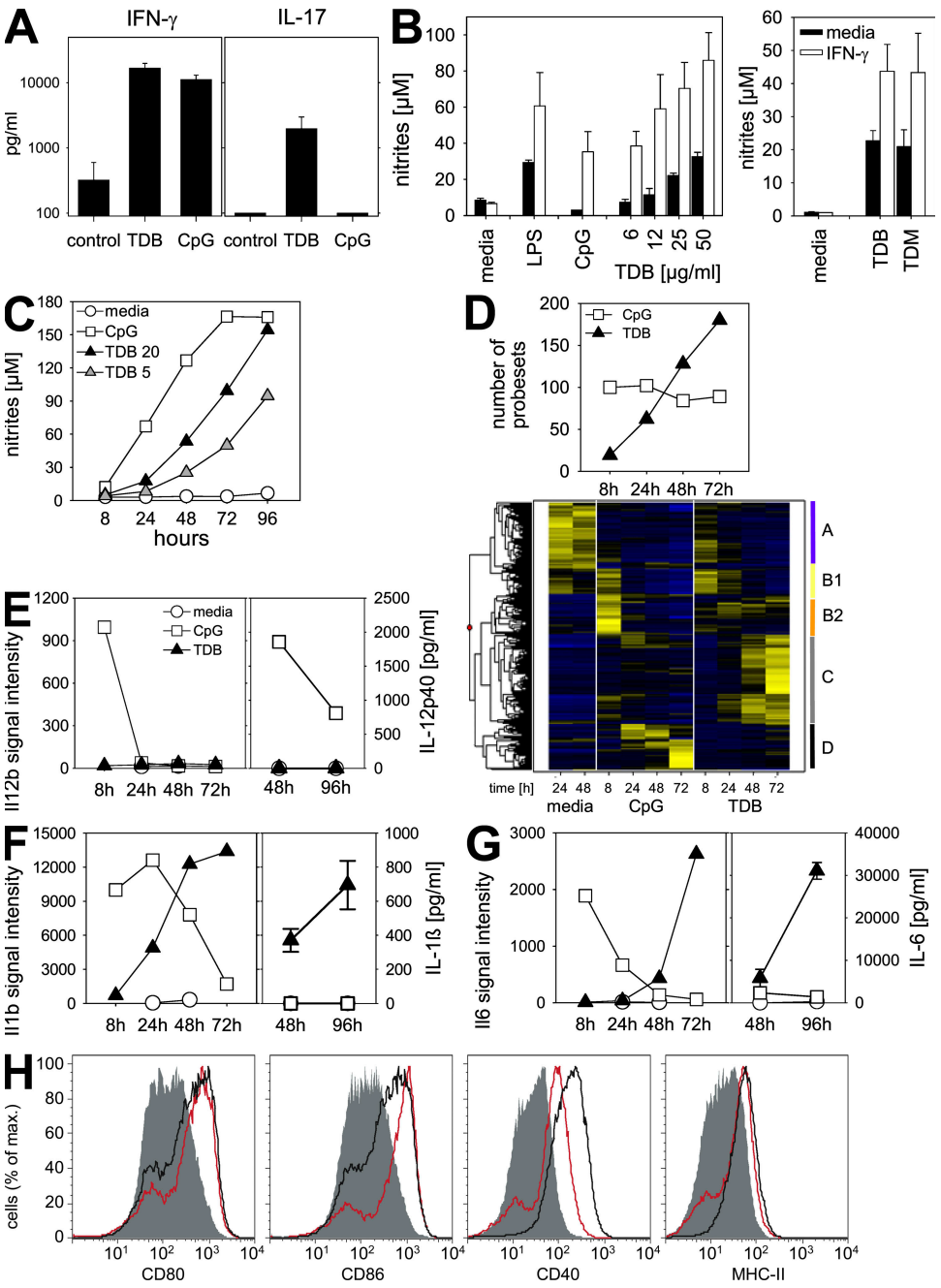

Figure 1. Th1/Th17 induction by TDB correlates with a distinct APC activation program. (A) C57BL/6 mice were s.c. immunized twice with H1 antigen mixed with CpG (CpG) or DDA-TDB (TDB) or left untreated (control). 2 wk after the last injection, draining lymph node cells were restimulated with 10 μg/ml H1 antigen for 96 h, followed by detection of IFN-γ and IL-17. Mean and SD (n = 3–4 mice) from representative experiment out of three are shown. (B) BMMs were stimulated for 96 h in triplicate with 100 ng/ml LPS, 1 μM CpG ODN, and TDB, with or without prestimulation with 20 ng/ml IFN-γ. NO production measured as nitrites by Griess assay. (right) TDB and TDM concentration of 20 μg/ml. Mean and SD of triplicate wells. (C) Stimulation of IFN-γ–primed BMMs as indicated. (D) Gene expression changes induced by TDB and CpG in IFN-γ–primed BMMs. (top) Number of probe sets up-regulated by >10-fold. (bottom) Hierarchical cluster analysis of z-score–normalized expression of regulated probe sets (Max-Min>200, Max/Min>10). Yellow indicates high, blue indicates low relative expression. (E–G) Cytokine mRNA and ELISA protein data. *Il12b* averages of probe sets 1449497_at and 1419530_at; *Il1b* probe set 1449399_a_at; *Il6* probe set 1450297_at. ELISA data are from triplicate wells. (H) Up-regulation of CD80, CD86, CD40, and MHC-II on DCs after stimulation with 30 μg/ml TDB (48 h; red line) or 100 ng/ml LPS (24 h; black line) compared with unstimulated cells (gray shade) as determined by FACS analysis. Representative of two experiments.

BMMs (Fig. S3). Thus, the adjuvant TDB potently activates APCs, in which it triggered a different expression program compared with TLR stimulation and presumably activates a distinct intracellular signaling pathway.

Requirement for Syk and Card9 in TDB-/TDM-induced APC activation

Diverse pattern recognition receptor families use different proximal signaling proteins to mediate myeloid cell activation. Whereas most TLRs signal via the adaptor protein MyD88 (3), certain ITAM receptors or ITAM-coupled receptors like C-type lectins use the kinase Syk for downstream signaling (14). To study whether any of these pathways are required for TDB-mediated cell activation we used MyD88$^{-/-}$ and Syk$^{-/-}$ BMMs (Fig. 2, A and B). As expected, control stimulation with TLR agonists resulted in normal production of NO in Syk$^{-/-}$ cells, but was ineffective in MyD88$^{-/-}$ BMMs. In contrast, TDB and TDM induced NO production in MyD88$^{-/-}$ cells to a similar extent as in wild-type cells, but did not stimulate NO synthesis in the absence of Syk. Furthermore, the TDB-stimulated expression and production of IL-6 by Myd88$^{-/-}$ BMMs was largely intact (Fig. S4, available at http://www.jem.org/cgi/content/full/jem.20081445/DC1), whereas Syk$^{-/-}$ BMMs failed to produce IL-6 and -1β (Fig. S5). As the small molecule Syk inhibitor Piceatannol blocked NO release induced by TDB and TDM from BMMs in a dose-dependent fashion (Fig. 2 C and Fig. S6), the enzymatic function of Syk is essential for the Myd88-independent innate immune cell activation in response to these glycolipids in vitro. Interestingly, Geisel et al. reported that Myd88 is required for cord factor–induced inflammation in vivo (9). Further, we have recently found that Myd88 is required for the Th1-directing adjuvant effect of TDB in vivo (15). Because TLR2, TLR3, TLR4, and TLR7 were not required (15), the phenotype of Myd88 knockout mice in vivo may indicate a defect in the glycolipid-induced effector phase, e.g., downstream of the IL-1 receptor.

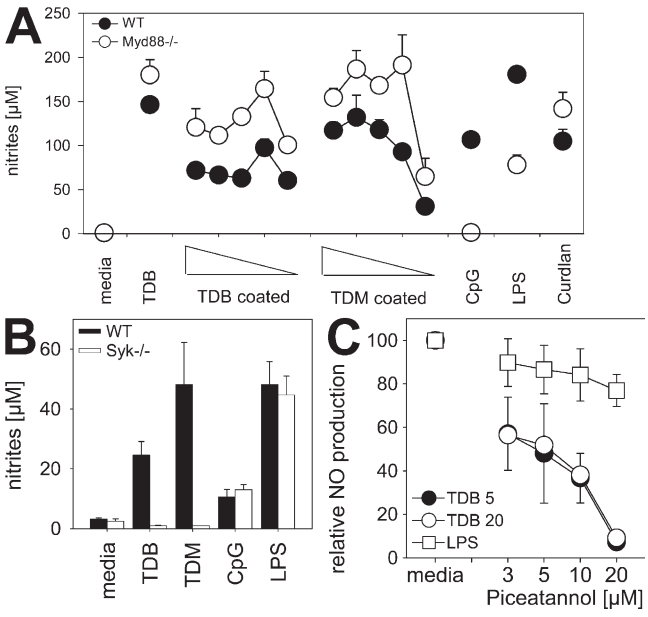

Figure 2. TDB-/TDM-induced APC activation is independent of Myd88, yet requires Syk activity. (A and B) Wild-type, Myd88$^{-/-}$, and Syk$^{-/-}$ BMMs primed with IFN-γ were stimulated for 60 h (A) and 96 h (B) before NO release was measured. TDB and TDM were used at 20 µg/ml in suspension (A and B) and coated onto tissue culture plastic in titrations ranging from 4 µg/ml to 15 ng/ml (A). Mean and SD of triplicate wells. Experiments were repeated three times with similar results. (C) TDB-induced macrophage activation is sensitive to Piceatannol. IFN-γ–primed BMMs were pretreated for 30 min with increasing doses of Piceatannol before stimulation with TDB (5 or 20 µg/ml) or LPS (100 ng/ml). Mean and SD of triplicate wells. Representative of two experiments.

Syk can use the myeloid cell–specific adaptor protein Card9 for the activation of macrophages or DCs in response to various signals (4–6). We therefore used Card9$^{-/-}$ BMMs to test whether APC activation by TDB requires this adaptor protein. Similar to Syk$^{-/-}$ BMMs, cells lacking Card9 failed to produce NO in response to TDB (Fig. S7, available at http://www.jem.org/cgi/content/full/jem.20081445/DC1) and to up-regulate expression of iNOS, IL-6, or IL-1β, whereas the CpG-mediated expression of these molecules was largely unaffected (Fig. 3 A). Gene expression profiling was used to determine whether Card9 is required for all transcriptional responses to TDB stimulation (Fig. 3 B). The β-glucan Curdlan, which is a ligand of the C-type lectin receptor Dectin-1 that is known to signal via Card9 (5), and TDB induced very similar genome-wide transcriptional responses that were distinct from the pattern of CpG-induced activation. In the absence of Card9, responses to TDB and Curdlan were almost completely abrogated, whereas CpG-triggered gene expression was unaffected. To further study the function of Card9 in TDB-induced APC activation, we also analyzed DCs and found that the release of IL-1β, IL-6, and TNF-α, as well as nuclear translocation of the transcription factor NF-κB, was triggered by TDB in a strictly Card9-dependent manner (Fig. S8 and Fig. S9). In contrast to BMMs (Fig. 1 E), DCs also produced IL-12p40 after stimulation with TDB or Curdlan, as well as IL-12p70 and -23, which are all dependent on Card9 (Fig. 3 C). Notably, LPS was a far stronger inducer of these Th differentiation factors than TDB (Fig. 3 C). Curdlan was comparably weak in IL-12 induction, in agreement with a previous study (5). It is known that Card9 can couple to the downstream adaptor and scaffold proteins Bcl10 and Malt1 (4). Using TNF-α production by DCs as readout for Bcl10 and Malt1 signaling, we found an additional requirement for these molecules in the response to TDB and TDM (Fig. 3 D). Thus, these experiments demonstrate on a genetic and transcriptional level that TDB and TDM engage a specific innate pathway that depends on Syk kinase activity and the adaptor proteins Card9, Bcl10, and Malt1.

TDB/TDM activate APCs independent of Dectin-1, yet require the ITAM-bearing adaptor protein FcRγ

As the β-glucan receptor Dectin-1 has already been implicated in APC responses to whole mycobacteria (16–18),

we tested its role in recognition of the mycobacterial cord factor TDM or TDB by APC. Using IFN-γ–primed Dectin-1$^{-/-}$ BMMs, we found the expected defect in NO production after stimulation with Curdlan, but the response to TDB and TDM, as well as to the TLR stimuli CpG and LPS, was not affected (Fig. 3 E). In addition, the expression of Nos2 and IL-1β after stimulation with TDB, TDM, and LPS was independent of Dectin-1 (Fig. S10, available at http://www.jem.org/cgi/content/full/jem.20081445/DC1). Thus, Dectin-1 is not required for TDB-/TDM-induced macrophage activation. In contrast to Dectin-1, which possesses an ITAM-like motif in its cytoplasmic region, a large number of Syk-activating myeloid cell receptors are associated with one of the ITAM-bearing adaptor proteins Dap12 or FcRγ (encoded by the *Fcer1g* gene). To gain further insight into the signaling requirements of APC activation by TDB and TDM, we used Dap12$^{-/-}$ and Fcer1g$^{-/-}$ BMMs (Fig. 3, F and G). Expression of Nos2 was independent of Dap12 in response to TLR ligands, Curdlan, and TDB/TDM. In contrast, in Fcer1g$^{-/-}$, BMM expression

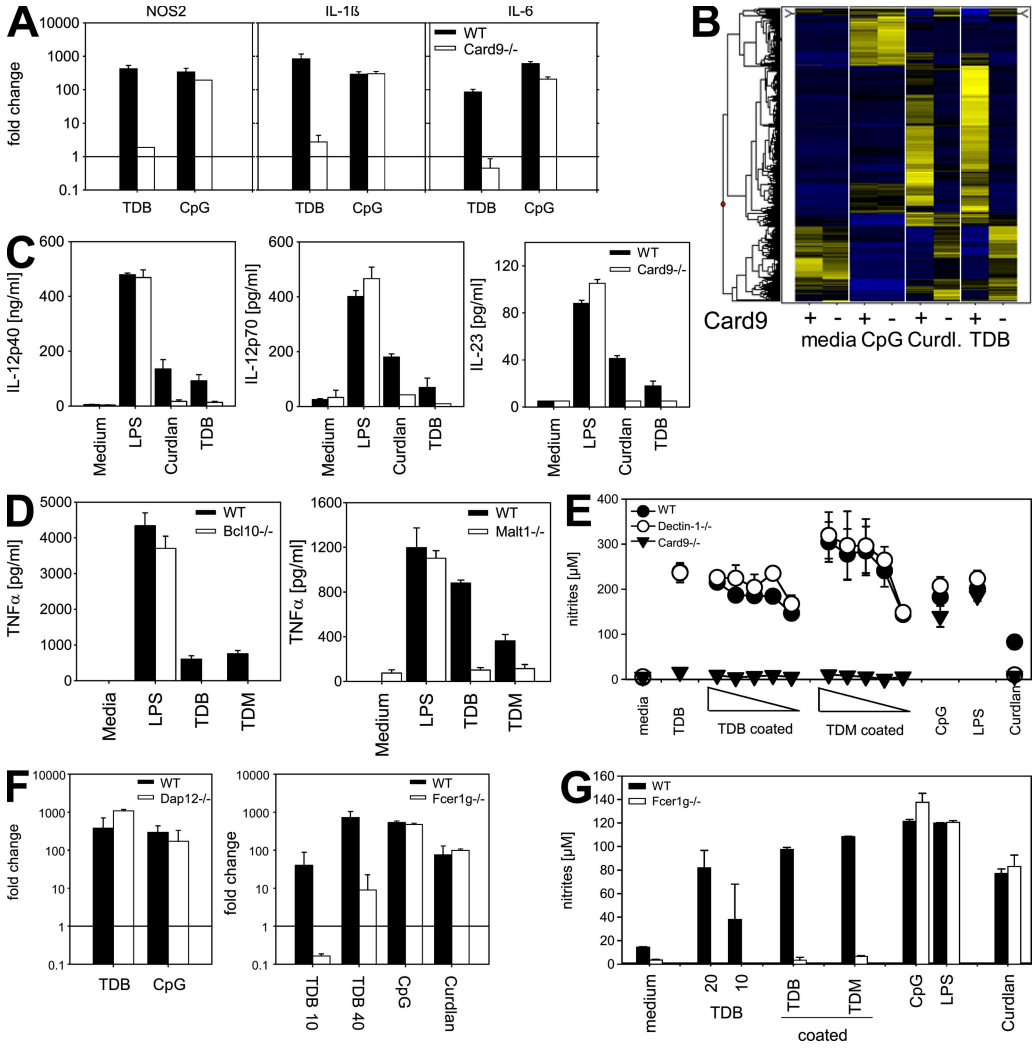

Figure 3. TDB/TDM activate APCs via Card9–Bcl10–Malt1. (A) BMM were stimulated with 1 µM CpG or 40 µg/ml TDB for 72 h. Expression of iNOS, IL-1β, and IL-6 was determined by qRT-PCR. Mean and SD of quadruplicate wells, representative of three independent experiments. (B) Expression profiling of wild-type and Card9$^{-/-}$ IFN-γ–primed BMMs 48 h after stimulation with CpG, TDB, or Curdlan. Hierarchical clustering of 606 probe sets with regulated expression (Max/Min > 5, Max-Min > 100). Yellow indicates high expression, blue indicates low relative expression. The genotype of BMMs is indicated with + (wild type) and – (Card9$^{-/-}$). (C) Card9 dependence of TDB-induced production of IL-12p40, IL-23, and IL-12p70 from DCs. LPS and Curdlan were included as controls. Shown are mean and SD of triplicate cultures, harvested 72 h after stimulation. (D) Lack of TNF-α production from DCs deficient in Bcl10 or Malt1. Mean and SD, repeated twice. (E) IFN-γ–primed BMMs from Dectin-1$^{-/-}$, Card9$^{-/-}$, and C57BL/6 mice were stimulated in triplicates for 72 h, as described in Fig. 2 A, before measurement of nitrites using the Griess assay. Mean and SD of representative experiment from two performed. (F) Expression of Nos2 mRNA in IFN-γ–primed BMMs from C57BL/6, Dap12$^{-/-}$, and Fcer1g$^{-/-}$ mice 48 h after stimulation as indicated. Fold change relative to medium control. Mean and SD of quadruplicate determinations, representative of at least two experiments. (G) NO production by C57BL/6 and Fcer1g$^{-/-}$ IFN-γ–primed BMMs 72 h after stimulation as indicated. Mean and SD of triplicate wells. Representative of three experiments.

of Nos2 and production of NO were specifically abrogated after stimulation with TDB or TDM, whereas TLR-triggered and Dectin-1–induced activation was intact. The specific requirement for FcRγ, but not Dap12, was also found for TDB-/TDM-induced expression of IL-6 (Fig. S11). Therefore, the ITAM-bearing adaptor FcRγ is critical for linking TDB and TDM recognition to the Syk–Card9 signaling pathway.

Lack of TDB-/TDM adjuvant activity in Card9$^{-/-}$ mice

The Syk–Card9 pathway is a pattern recognition pathway that can couple to adaptive immunity (5). To investigate whether

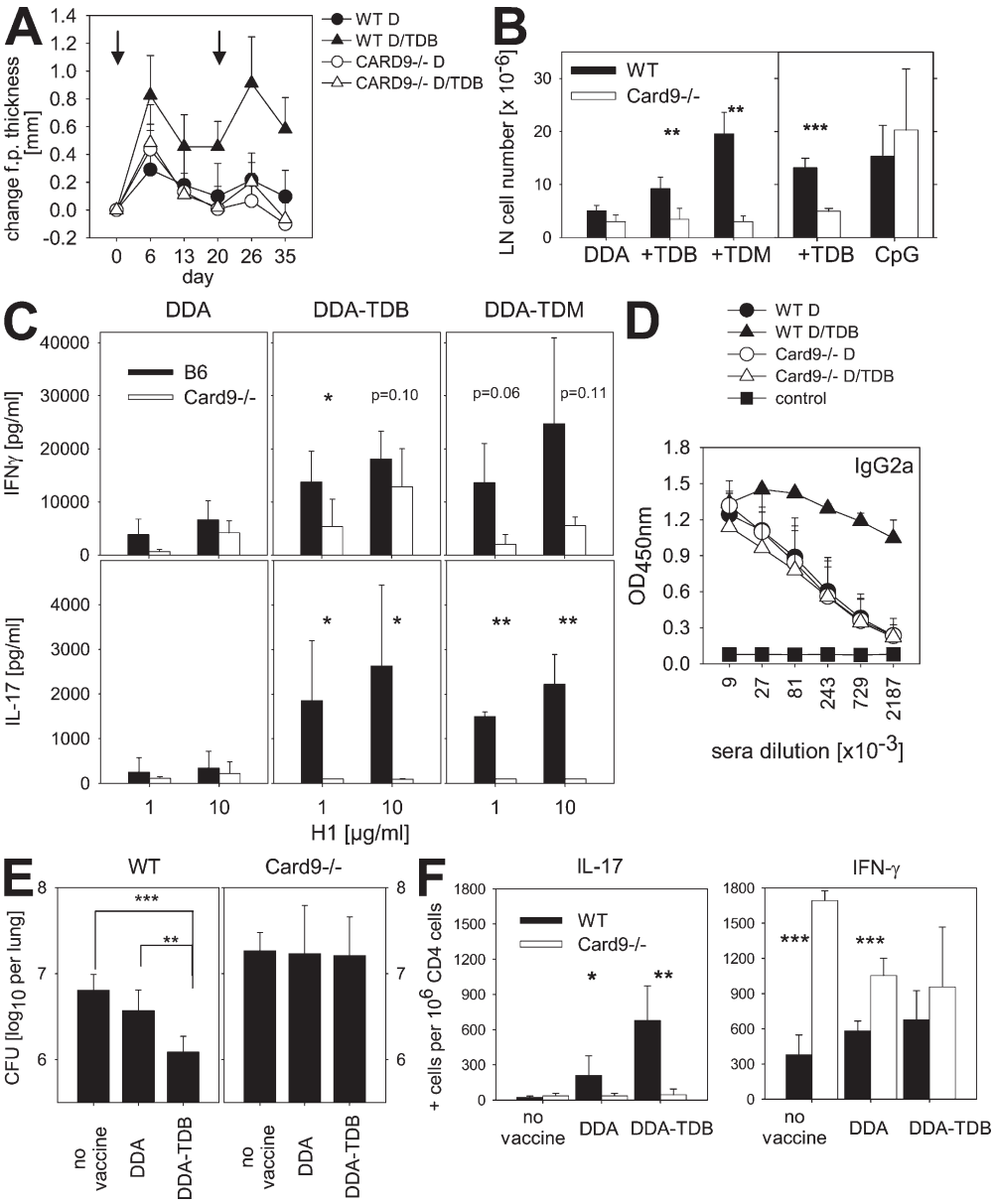

Figure 4. Induction of protective immunity to tuberculosis by TDB/TDM adjuvant requires Card9. (A) Wild-type and Card9$^{-/-}$ mice were immunized via hind footpad injection on day 0 and 20 (arrows) with H1 in DDA or DDA/TDB liposomes. Mean and SD of the increase in footpad thickness is shown (footpad number, $n = 12$). Significantly different for comparison of wild-type and Card9$^{-/-}$ after DDA/TDB injection at all time points ($P < 0.01$). Representative of two independent experiments. (B) Number of cells in draining lymph nodes 2 wk after the 2 injections. Data are from two independent experiments ($n = 3$–5 for each data point). (C) Production of IFN-γ and IL-17 by draining lymph node cells after restimulation with H1 protein. Mean and SD ($n = 4$), two experiments with similar results. (D) IgG2a levels in sera of mice injected three times. Control, untreated mice; D, DDA; *D/T:* DDA/TDB; WT, wild type. (E) Mice injected three times, or naive mice, were infected by aerosol with 100 CFU MTB. After 6 wk, mice were killed and the bacterial load was determined in the lung. (left) Wild-type mice; (right) Card9$^{-/-}$ mice. Shown are mean and SD from six mice per group, except for unvaccinated Card9$^{-/-}$ mice, where two mice died before day 42. (F) Frequency analysis of CD4 T cells producing IL-17 (left) or IFN-γ (right) from mediastinal lymph nodes 6 wk after MTB infection. Asterisks indicate significant differences (*, $P < 0.05$; **, $P < 0.01$; ***, $P < 0.001$).

this innate pathway is responsible for the adjuvant activity of TDB in vivo, we immunized Card9$^{-/-}$ animals with H1 and TDB or TDM. Card9-deficient mice were used as they have selective defects in myeloid cells but intact lymphocyte activation, in contrast to Syk$^{-/-}$, Bcl10$^{-/-}$, and Malt1$^{-/-}$ animals (4, 19). Although the transient footpad swelling after injection of H1 in liposomes alone was comparable between wild-type and Card9$^{-/-}$ mice, the inclusion of TDB (Fig. 4 A) or TDM (not depicted) into the liposomes caused an increase in footpad thickness that was completely abrogated in Card9-deficient mice. Moreover, TDB and TDM injection augmented draining lymph node cellularity in wild-type but not Card9$^{-/-}$ mice, whereas the response to CpG was comparable between the two genotypes (Fig. 4 B). The TDM- or TDB-induced capacity of lymph node cells for IFN-γ production was reduced in Card9$^{-/-}$ mice, indicating that Th-1 differentiation directed by these glycolipids depends on Card9 (Fig. 4 C). The development of a H1-specific IL-17 production conferred by TDB and TDM was completely abrogated, suggesting a crucial role of the Syk–Card9 pathway for TDB-/TDM-induced Th-17 differentiation (Fig. 4 C). Moreover, H1-specific IgG2a antibody levels were Card9 dependently enhanced by TDB (Fig. 4 D). Thus, using different readout systems for Th-1, Th-17, and antibody responses, we find that Card9 is essential to mediate the adjuvanticity of TDB and TDM in vivo.

To test whether Card9 signaling is also responsible for the immune protection after subunit vaccination with H1 plus TDB, which confers a similar reduction in pulmonary mycobacterial load as the live BCG vaccine (13), we challenged immunized mice with low-dose aerosol MTB infection and analyzed CFUs in the organs 6 wk later. As expected, compared with naive mice, vaccination with H1 in TDB-containing liposomes caused a significant reduction of mycobacterial load in the lungs of wild-type mice, whereas the liposomes alone had no significant effect (Fig. 4 E). In sharp contrast, immunization with TDB and H1 failed to reduce the number of mycobacterial CFUs in the lungs of Card9$^{-/-}$ mice, demonstrating a key role of Card9-signaling in TDB-induced protective immunity against tuberculosis in vivo. This protective effect correlated with the Card9-dependent induction of antigen-specific Th-17 cells in the mediastinal lymph nodes after vaccination, but not with the frequency of H1-specific IFN-γ–producing CD4$^+$ T cells (Fig. 4 F). Notably, lung mycobacterial load in nonimmunized Card9$^{-/-}$ mice was higher than in wild types ($P < 0.01$), suggesting an additional role for the Card9 pathway in the natural resistance to MTB infection that deserves further detailed investigation and that could explain the substantially elevated numbers of IFN-γ–producing T cells in Card9$^{-/-}$ mice (Fig. 4 F).

Concluding remarks

In conclusion, we report the molecular pathway for the adjuvanticity of TDM and TDB by demonstrating that these glycolipids specifically activate APCs via Syk–Card9–Bcl10–Malt1 signaling. The precise receptor(s) that recognize(s) TDB or TDM remain(s) to be determined. As we have excluded an essential role of Dectin-1, its contribution to the activation of APCs by whole mycobacteria (16–18) is likely caused by mycobacterial ligands distinct from TDM. Given the multitude of receptors that can activate Syk–Card9 in myeloid cells, our finding that the ITAM-bearing adaptor FcRγ, but not Dap12, is essential for activation of macrophages by TDB and TDM provides a starting point for the isolation of pattern recognition receptors for these mycobacterial glycolipids. Although Dap12-coupled molecules like TREMs, Sirpb, and PILR-b are unlikely to be involved, some C-type lectins (e.g., Mincle, Dectin-2, and DCAR), as well as other FcRγ-coupled proteins (e.g., OSCAR and PIRA), can be considered candidate receptors.

Our results further indicate that TDB and TDM constitute adjuvants with a now molecularly defined mode of action that is distinct from TLR-triggering adjuvants engaging Myd88 (CpG and IC31) (20–22) or Trif (Monophosphoryl Lipid A) (23). It is intriguing that the innate activation program induced by the mycobacterial cord factor and its analogue TDB instructs the development of the appropriate, protective Th-1 and -17 response. Consistent with recent findings that established the importance of Th-17 cells after subunit vaccination using a TDM-containing adjuvant (8), the degree of Th-17 cell induction correlated with protection to MTB-challenge in our experiments. According to the current concept of murine and human Th-17 differentiation (24, 25), TDB likely operates through the combined induction of IL-1β, -6, and -23 from APCs, whereas CpG may inhibit Th-17 differentiation through IL-12 and IFN-γ (5, 25). Our finding that the glycolipid adjuvants TDB and TDM mediate their protective effects via Syk–Card9 signaling provides a rational basis for the further development of efficient TB immunization strategies.

MATERIALS AND METHODS

Mice. C57BL/6 mice were purchased from Harlan-Winkelmann. Breeding pairs for mice deficient in Myd88 were provided by S. Akira (Research Institute for Microbial Diseases, Osaka, Japan). Card9$^{-/-}$, Bcl10$^{-/-}$, and Malt1$^{-/-}$ mice have been previously described (4, 19). All knockout mice used for immunization experiments were backcrossed to C57BL/6 for at least six generations. Syk$^{+/-}$ mice were provided by V. Tybulewicz (National Institute for Medical Research, London, England, UK). Syk$^{-/-}$ and Syk$^{+/+}$ fetal liver cells were used to generate BM radiation chimeras. Dap12$^{-/-}$ and Fcer1g$^{-/-}$ mice were used with permission from T. Takai (26, 27). Dectin1$^{-/-}$ mice have been previously described (28). Animal experiments were approved by the Regierung von Oberbayern (AZ209.1/211-2531-33/05) and the Animal Research Ethics Board of the Ministry of Environment, Nature Protection and Agriculture, Kiel, Germany.

Reagents. CpG ODN 1826 has been previously described (21) and was supplied in phosphorothioate form by Coley Pharmaceuticals. *E. coli* O55:B5 LPS was obtained from Sigma-Aldrich. TDB was purchased from Sigma-Aldrich or Avanti Polar Lipids. TDM was purchased from Sigma-Aldrich or Axxora. The purity of TDB and TDM was confirmed by mass spectrometry. For preparation of liposomes, dimethyldioctadecylammonium (DDA) bromide and TDB were purchased from Avanti Polar Lipids. The fusion protein of Ag85B and ESAT-6 (designated H1) was produced as a recombinant protein, as previously described (29). Piceatannol (Calbiochem) was solubilized in DMSO. Curdlan was purchased from Wako Chemicals. IFN-γ was purchased from Tebu-Bio.

Generation of macrophages and dendritic cells. Macrophages were differentiated from BM cells in cDMEM containing 10% L-cell conditioned medium for 6–7 d. After removal of nonadherent cells, macrophages were detached from Petri dishes using Accutase treatment, washed, counted, and replated at a density of 10^6 cells/ml. Macrophages were rested overnight before stimulation, as indicated in the figure legends. Where indicated, cells were pretreated for 3 h with IFN-γ at a concentration of 10 ng/ml. For generation of BMDC, BM cells were cultured on Petri dishes for 7 d in cRPMI containing 20 ng/ml of GM-CSF (Peprotech). The cells were plated at a density of 5×10^5 cells/ml and stimulated as indicated in the figure legends.

Stimulation of macrophages with TDB and TDM. Stocks of the glycolipids TDB and TDM were prepared by solubilizing in PBS with 2% DMSO by alternating vortexing and heating to 50°C at a concentration of 2.5 mg/ml. Macrophages were stimulated using 1–50 μg/ml TDB or TDM as indicated in figure legends. In some experiments, the glycolipids were coated directly to the bottom of cell culture plates after the procedure described by Ozeki et al. (30). In brief, 2.5 mg/ml TDB or 1 mg/ml TDM were dissolved in isopropanol by heating to 60°C for 20 min, followed by vortexing for 5 min. The glycolipids were coated in a volume of 20 μl for 96-well plates and 40 μl for 48-well plates. Concentrations were calculated by dividing the amount of TDB/TDM in the wells by the culture medium volume.

Measurement of NO and cytokines. The Griess assay was used to determine the reaction products of NO in culture supernatants of stimulated macrophages. Levels of cytokines were measured by sandwich ELISA using antibody pairs from R&D Systems.

RNA isolation. Total RNA was prepared from stimulated macrophages using RNeasy Mini kit (QIAGEN) and measured on a Nanodrop spectrophotometer. RNA samples used for microarray analysis were quality controlled for integrity of the RNA using Bio-Rad Experion Standard Sensitivity Chips (Bio-Rad Laboratories).

Microarray analysis. Affymetrix GeneChips were used for genome-wide transcriptome analysis of 1 μg total RNA per sample, following the manufacturer's instruction for labeling and hybridization of the samples. In the first experiment measuring the kinetics of changes induced by CpG or TDB in Fig. 1, samples were processed using the GeneChip Expression 3′ Amplification One-Cycle Target Labeling kit. Biotinylated cRNA was then hybridized on MOE430 2.0 GeneChips that were stained, washed, and scanned after standard procedures. In the second experiment, comparing wild-type and $Card9^{-/-}$ macrophages after a 48-h stimulation with CpG, Curdlan, and TDB (Fig. 3), samples were processed with the Whole Transcript Assay kit and hybridized to Mouse Gene 1.0 ST GeneChips, as detailed by the manufacturer. CEL files were processed for global normalization and generation of expression values using the robust multi-array average algorithm. To select regulated genes, the data were filtered by excluding all probe sets that over all conditions showed <10-fold (Fig. 1) or <5-fold (Fig. 3) change and an absolute difference between maximum and minimum expression values of <200 (Fig. 1) or <100 (Fig. 3). The probe sets passing these criteria were z-score normalized and subjected to hierarchical clustering using Spotfire DecisionSite Functional Genomics software. Tables S1 and S2 (available at http://www.jem.org/cgi/content/full/jem.20081445/DC1) list the expression data for the probe sets shown in Fig. 1 D and Fig. 3 D, respectively. The Cel files for both experiments were submitted to the public repository Gene Expression Omnibus (Accession nos. GSE10530 and GSE10532).

Quantitative RT-PCR. Expression levels of the housekeeping gene HPRT, the cytokines IL-6 and -1β, and iNOS were analyzed using primer/probe combinations selected from the Roche Universal Probe Library and are available upon request. Fold changes were calculated with the ΔΔCT method using the untreated sample as a calibrator.

Immunization of mice with Ag85B–ESAT-6 fusion protein H1. Groups of 3–6 mice were immunized subcutaneously by footpad injection 2 or 3 times, with a 2-wk interval between injections. All mice were immunized with 2 μg of the vaccine antigen H1 emulsified in 100 μl of each adjuvant (50 μl per foot), comprising either 250 μg DDA liposomes alone, 250 μg DDA + 50 μg TDB, or 250 μg DDA + 50 μg TDM. DDA was suspended in sterile distilled water at 2.5 mg/ml, heated to 80°C for 20 min with continuous stirring in order for liposomes to form, and left to cool at room temperature. A stable formulation of DDA/TDB was prepared by the lipid film hydration method, as previously described (12). TDM was suspended in sterile distilled water containing 2% dimethylsulfoxide to a concentration of 5 mg/ml by repeated passaging through a fine-tipped pipette, followed by vortexing. This step was repeated 3 times before freezing the solution at −20°C until use. Before immunization, H1 was mixed in Tris buffer and TDM was added and finally mixed with DDA. For immunization with CpG as adjuvant, H1 was mixed in PBS with the ODN such that one dose (per footpad) contained 2 μg H1 protein and 5 nmol CpG.

Footpad thickness was determined with a caliper before and at several time points after injection. Baseline values were subtracted individually for both feet of each mouse.

Measurement of antigen-specific production of IFN-γ and IL-17. 4 wk after the first immunization, the draining lymph nodes of the mice were removed and passed through a 100-μm nylon cell strainer (BD). For restimulation, 3×10^5 cells (in a total volume of 250 μl RPMI) were plated in triplicate in 96-well culture plates. H1 antigen was used at 1 μg/ml and 10 μg/ml final concentrations for restimulation. Wells containing medium only or 1 μg/ml ConA were used as negative and positive controls, respectively. Culture supernatants were harvested after 96 h incubation, and the amount of IFN-γ and IL-17 was determined by ELISA.

Determination of antigen-specific antibody responses. To evaluate the presence of H1-specific antibodies, mouse sera of the immunized mice were analyzed in triplicate in threefold dilutions (beginning at a 1/1,000 dilution). Reagents used for determining specific antibody titers were rabbit anti–mouse IgG1 and $IgG2a^b$ (BD). Absorbance was read on an ELISA reader at 450 nm.

Low-dose aerosol MTB challenge. Before infection of experimental animals, stock solutions of MTB H37rv were diluted in sterile distilled water and pulmonary infection with 100 CFU/lung was performed using an inhalation exposure system (Glas-Col). 6 wk after infection, mice were sacrified to aseptically remove lungs and mediastinal lymph nodes. To determine bacterial loads, lungs were weighed and homogenized in PBS containing a proteinase inhibitor cocktail (Roche). 10-fold serial dilutions of organ homogenates were plated in duplicates onto Middlebrook 7H10 agar plates containing 10% OADC and incubated at 37°C for 19–21 d. Colonies on plates were enumerated and results expressed as $\log_{10}$ CFU per organ. To analyze the frequency of Th-1 and -17 cells, CD4 T cells from mediastinal lymph nodes were enriched by magnetic cells sorting (Miltenyi). Detection of antigen-specific IFN-γ– and IL-17–producing CD4 T cells was conducted using ELISPOT assay kits from BD and R&D Systems, respectively. Doubling dilutions of CD4 T cells were incubated with mitomycin-D–inactivated (Sigma-Aldrich) splenocytes from uninfected wild-type mice and were restimulated with H1 at a concentration of 10 μg/ml in the presence of 10 U/ml recombinant mouse IL-2 (Peprotech). After development, spots were automatically enumerated using an ELISPOT reader (ELISpot 04 XL; AID Diagnostika), and the frequency of responding CD4 T cells was determined.

Online supplemental material. Fig. S1 gives the chemical structures of TDB and TDM. Fig. S2 depicts validation of microarray data. Fig. S3 shows production of TNF-α and NO by DCs in response to TDB and TDM. Myd88-independent expression and secretion of IL-6 by TDB-stimulated macrophages is shown in Fig. S4. Fig. S5 shows IL-6 and -1b ELISA data from Syk-deficient macrophages. Inhibition of TDB- and TDM-induced NO release by Piceatannol is depicted in Fig. S6. Fig. S7 depicts Card9-dependent NO production by macrophages. Fig. S8 shows the expression of cytokines in DCs in response to TDB. Fig. S9 is a NF-κB EMSA showing Card9-dependent activation in DCs. Fig. S10 gives qPCR data showing Dectin1-independent expression of iNOS, IL-1β, and

IL-6 in response to TDB and TDM. Fig. S11 compares the requirement for *Dap12* and *Fcer1g* in TDB-induced expression of IL-6. Online supplemental material is available at http://www.jem.org/cgi/content/full/jem.20081445/DC1.

Technical support by Barbara Bodendorfer and Angela Servatius is highly appreciated.

Work in the authors' laboratories is funded by grants from Deutsche Forschungsgemeinschaft (SFB-576 to J. Ruland, R. Lang, and H. Wagner; SFB 643 to F. Nimmerjahn and R. Lang; and HO 2145/3-1 to C. Hölscher), Max-Eder Programm der Deutschen Krebshilfe (J. Ruland), Bundesministerium für Bildung und Forschung (EXC306 to C. Hölscher), Bayerisches Genomforschungsnetz (F. Nimmerjahn), the Hungarian National Office for Research and Technology (grant NKFP-A1-2006-0069 to A. Mocsai), and the European Commission FP6 (TB-VAC grants to E.M. Agger, P. Andersen, H. Wagner, and R. Lang).

Potential conflict of interest: P. Andersen is a co-inventor of patents relating to cationic liposomes as vaccine adjuvants. The other authors have no competing financial interests.

Submitted: 3 July 2008
Accepted: 15 December 2008

REFERENCES

1. Kaufmann, S.H. 2006. Envisioning future strategies for vaccination against tuberculosis. *Nat. Rev. Immunol.* 6:699–704.
2. Andersen, P., and T.M. Doherty. 2005. The success and failure of BCG - implications for a novel tuberculosis vaccine. *Nat. Rev. Microbiol.* 3:656–662.
3. Akira, S., and K. Takeda. 2004. Toll-like receptor signalling. *Nat. Rev. Immunol.* 4:499–511.
4. Gross, O., A. Gewies, K. Finger, M. Schafer, T. Sparwasser, C. Peschel, I. Forster, and J. Ruland. 2006. Card9 controls a non-TLR signalling pathway for innate anti-fungal immunity. *Nature.* 442:651–656.
5. LeibundGut-Landmann, S., O. Gross, M.J. Robinson, F. Osorio, E.C. Slack, S.V. Tsoni, E. Schweighoffer, V. Tybulewicz, G.D. Brown, J. Ruland, and C. Reis e Sousa. 2007. Syk- and CARD9-dependent coupling of innate immunity to the induction of T helper cells that produce interleukin 17. *Nat. Immunol.* 8:630–638.
6. Hara, H., C. Ishihara, A. Takeuchi, T. Imanishi, L. Xue, S.W. Morris, M. Inui, T. Takai, A. Shibuya, S. Saijo, et al. 2007. The adaptor protein CARD9 is essential for the activation of myeloid cells through ITAM-associated and Toll-like receptors. *Nat. Immunol.* 8:619–629.
7. Flynn, J.L., J. Chan, K.J. Triebold, D.K. Dalton, T.A. Stewart, and B.R. Bloom. 1993. An essential role for interferon γ in resistance to *Mycobacterium tuberculosis* infection. *J. Exp. Med.* 178:2249–2254.
8. Khader, S.A., G.K. Bell, J.E. Pearl, J.J. Fountain, J. Rangel-Moreno, G.E. Cilley, F. Shen, S.M. Eaton, S.L. Gaffen, S.L. Swain, et al. 2007. IL-23 and IL-17 in the establishment of protective pulmonary CD4(+) T cell responses after vaccination and during *Mycobacterium tuberculosis* challenge. *Nat. Immunol.* 8:369–377.
9. Geisel, R.E., K. Sakamoto, D.G. Russell, and E.R. Rhoades. 2005. In vivo activity of released cell wall lipids of *Mycobacterium bovis* bacillus Calmette-Guerin is due principally to trehalose mycolates. *J. Immunol.* 174:5007–5015.
10. Lima, K.M., S.A. Santos, V.M. Lima, A.A. Coelho-Castelo, J.M. Rodrigues Jr., and C.L. Silva. 2003. Single dose of a vaccine based on DNA encoding mycobacterial hsp65 protein plus TDM-loaded PLGA microspheres protects mice against a virulent strain of *Mycobacterium tuberculosis*. *Gene Ther.* 10:678–685.
11. Pimm, M.V., R.W. Baldwin, J. Polonsky, and E. Lederer. 1979. Immunotherapy of an ascitic rat hepatoma with cord factor (trehalose-6, 6'-dimycolate) and synthetic analogues. *Int. J. Cancer.* 24:780–785.
12. Davidsen, J., I. Rosenkrands, D. Christensen, A. Vangala, D. Kirby, Y. Perrie, E.M. Agger, and P. Andersen. 2005. Characterization of cationic liposomes based on dimethyldioctadecylammonium and synthetic cord factor from *M. tuberculosis* (trehalose 6,6'-dibehenate)-a novel adjuvant inducing both strong CMI and antibody responses. *Biochim. Biophys. Acta.* 1718: 22–31.
13. Holten-Andersen, L., T.M. Doherty, K.S. Korsholm, and P. Andersen. 2004. Combination of the cationic surfactant dimethyl dioctadecyl ammonium bromide and synthetic mycobacterial cord factor as an efficient adjuvant for tuberculosis subunit vaccines. *Infect. Immun.* 72:1608–1617.
14. Underhill, D.M., and H.S. Goodridge. 2007. The many faces of ITAMs. *Trends Immunol.* 28:66–73.
15. Agger, E.M., I. Rosenkrands, J. Hansen, K. Brahimi, B.S. Vandahl, C. Aagaard, K. Werninghaus, C. Kirschning, R. Lang, D. Christensen, et al. 2008. Cationic liposomes formulated with synthetic mycobacterial cord factor (CAF01): a versatile adjuvant for vaccines with different immunological requirements. *PLoS ONE.* 3:e3116.
16. Rothfuchs, A.G., A. Bafica, C.G. Feng, J.G. Egen, D.L. Williams, G.D. Brown, and A. Sher. 2007. Dectin-1 interaction with *Mycobacterium tuberculosis* leads to enhanced IL-12p40 production by splenic dendritic cells. *J. Immunol.* 179:3463–3471.
17. Shin, D.M., C.S. Yang, J.M. Yuk, J.Y. Lee, K.H. Kim, S.J. Shin, K. Takahara, S.J. Lee, and E.K. Jo. 2008. *Mycobacterium abscessus* activates the macrophage innate immune response via a physical and functional interaction between TLR2 and dectin-1. *Cell. Microbiol.* 10:1608–1621.
18. Yadav, M., and J.S. Schorey. 2006. The beta-glucan receptor dectin-1 functions together with TLR2 to mediate macrophage activation by mycobacteria. *Blood.* 108:3168–3175.
19. Ruland, J., and T.W. Mak. 2003. Transducing signals from antigen receptors to nuclear factor kappaB. *Immunol. Rev.* 193:93–100.
20. Agger, E.M., I. Rosenkrands, A.W. Olsen, G. Hatch, A. Williams, C. Kritsch, K. Lingnau, A. von Gabain, C.S. Andersen, K.S. Korsholm, and P. Andersen. 2006. Protective immunity to tuberculosis with Ag85B-ESAT-6 in a synthetic cationic adjuvant system IC31. *Vaccine.* 24:5452–5460.
21. Heit, A., F. Schmitz, T. Haas, D.H. Busch, and H. Wagner. 2007. Antigen co-encapsulated with adjuvants efficiently drive protective T cell immunity. *Eur. J. Immunol.* 37:2063–2074.
22. Kwissa, M., R.R. Amara, H.L. Robinson, B. Moss, S. Alkan, A. Jabbar, F. Villinger, and B. Pulendran. 2007. Adjuvanting a DNA vaccine with a TLR9 ligand plus Flt3 ligand results in enhanced cellular immunity against the simian immunodeficiency virus. *J. Exp. Med.* 204:2733–2746.
23. Mata-Haro, V., C. Cekic, M. Martin, P.M. Chilton, C.R. Casella, and T.C. Mitchell. 2007. The vaccine adjuvant monophosphoryl lipid A as a TRIF-biased agonist of TLR4. *Science.* 316:1628–1632.
24. Sutton, C., C. Brereton, B. Keogh, K.H. Mills, and E.C. Lavelle. 2006. A crucial role for interleukin (IL)-1 in the induction of IL-17–producing T cells that mediate autoimmune encephalomyelitis. *J. Exp. Med.* 203:1685–1691.
25. Harrington, L.E., R.D. Hatton, P.R. Mangan, H. Turner, T.L. Murphy, K.M. Murphy, and C.T. Weaver. 2005. Interleukin 17-producing CD4+ effector T cells develop via a lineage distinct from the T helper type 1 and 2 lineages. *Nat. Immunol.* 6:1123–1132.
26. Kaifu, T., J. Nakahara, M. Inui, K. Mishima, T. Momiyama, M. Kaji, A. Sugahara, H. Koito, A. Ujike-Asai, A. Nakamura, et al. 2003. Osteopetrosis and thalamic hypomyelinosis with synaptic degeneration in DAP12-deficient mice. *J. Clin. Invest.* 111:323–332.
27. Takai, T., M. Li, D. Sylvestre, R. Clynes, and J.V. Ravetch. 1994. FcR gamma chain deletion results in pleiotrophic effector cell defects. *Cell.* 76:519–529.
28. Taylor, P.R., S.V. Tsoni, J.A. Willment, K.M. Dennehy, M. Rosas, H. Findon, K. Haynes, C. Steele, M. Botto, S. Gordon, and G.D. Brown. 2007. Dectin-1 is required for beta-glucan recognition and control of fungal infection. *Nat. Immunol.* 8:31–38.
29. Olsen, A.W., A. Laurens, H. van Pinxteren, L.M. Okkels, P.B. Rasmussen, and P. Andersen. 2001. Protection of mice with a tuberculosis subunit vaccine based on a fusion protein of antigen 85B and ESAT-6. *Infect. Immun.* 69:2773–2778.
30. Ozeki, Y., H. Tsutsui, N. Kawada, H. Suzuki, M. Kataoka, T. Kodama, I. Yano, K. Kaneda, and K. Kobayashi. 2006. Macrophage scavenger receptor down-regulates mycobacterial cord factor-induced proinflammatory cytokine production by alveolar and hepatic macrophages. *Microb. Pathog.* 40:171–176.